# Structure of Lithium Nitride and Transition-Metal-Doped Derivatives, $Li_{3-x-y}M_xN$ (M = Ni, Cu): A Powder Neutron Diffraction Study

Duncan H. Gregory,*,† Paul M. O'Meara,† Alexandra G. Gordon,† Jason P. Hodges,‡ Simine Short,§ and James D. Jorgensen§

*School of Chemistry, University of Nottingham, Nottingham, NG7 2RD United Kingdom, Spallation Neutron Source Division, Oak Ridge National Laboratory, Oak Ridge, Tennessee 37830, and Materials Science Division, Argonne National Laboratory, Argonne, Illinois 60439*

*Received August 6, 2001. Revised Manuscript Received February 14, 2002*

Structures of lithium nitride (α-$Li_3N$) and ternary nitridometalates $Li_{3-x-y}M_xN$ (M = Ni, Cu) have been refined from time-of-flight powder neutron diffraction data using the Rietveld method. The parent binary nitride was synthesized by reaction of lithium metal with nitrogen using liquid sodium as a solvent. The ternary nitrides were prepared by reaction of $Li_3N$ with the respective transition metals under nitrogen. Refined data confirm the hexagonal structure previously reported by single-crystal X-ray diffraction for lithium nitride ($P6/mmm$, $a = 3.6576(1)$ Å, $c = 3.8735(1)$ Å, $Z = 1$) and show that the α-$Li_3N$ phase contains close to 3% Li vacancies at room temperature. The substituted nitridometalates, $Li_{1.36}Ni_{0.79}N$ and $Li_{2.21}Cu_{0.40}N$, both form structures analogous to α-$Li_3N$ ($P6/mmm$, $a = 3.7697(1)$ Å, $c = 3.5270(1)$ Å and $a = 3.6791(1)$ Å, $c = 3.7725(1)$ Å, respectively) in which the transition metal is disordered with Li between $[Li_{2-y}N]$ planes and Li vacancies are disordered within these planes. The nickel and copper nitrides contain 43% ($y = 0.85$) and 16% ($y = 0.32$) Li vacancies, respectively, within the $[Li_2N]$ planes and consequently contain transition metals predominantly in the +2 oxidation state.

## Introduction

Research in nitride chemistry has grown dramatically in recent years.[1] Advances in this area have been fundamental yet, increasingly, the emphasis has also been to investigate the physical properties of this growing array of unusual compounds in the search for novel non-oxide materials. Lithium nitride, $Li_3N$, is one such unusual compound and has formed the basis for a significant amount of work over several decades.[2−4] Not only is it the solitary stable alkali metal binary nitride, but it also has a unique layered structure.[5−7] Moreover, $Li_3N$ is a fast lithium ion conductor and a potential solid electrolyte in lithium batteries. Extensive studies illustrated that the conduction in $Li_3N$ is achieved via intrinsic defects (1−2% Li vacancies) in the $[Li_2N]$ planes of the structure and at ≈300 K involves a hopping mechanism of $Li^+$ exclusively within these planes (perpendicular to the *c* axis).[2−4,8] The largest perceived drawback to the application of $Li_3N$ as an electrolyte, however, is its relatively low decomposition potential (0.44 V).

Recently, attention has therefore shifted to ternary lithium nitride compositions in an effort to improve the stability of any prospective battery material. Subsequent studies in the quest for new lithium nitride battery materials have concentrated on two groups of ternary compounds—those forming anti-fluorite structures, $[Li_{2-x-y}\square_yM_xN]_n$ (□ = Li vacancy, M = Fe, Al, Si, for example)[9,10] and those derived from lithium nitride itself, $Li_{3-x}M_xN$ (M = Co, Ni, Cu).[11−13] Electrochemical testing of compounds in the Li−Co−N system, for example, identifies these nitrides as promising anode materials in lithium secondary batteries, with good cycleability and a volumetric capacity significantly superior to graphite.[13−16]

* To whom correspondence should be addressed. E-mail: Duncan.Gregory@Nottingham.ac.uk.
† University of Nottingham.
‡ Oak Ridge National Laboratory.
§ Argonne National Laboratory.

(1) See for example: (a) Gregory, D. H. *J. Chem. Soc., Dalton Trans.* **1999**, 259. (b) Niewa, R.; DiSalvo, F. J. *Chem. Mater.* **1998**, *10*, 2733.
(2) v. Alpen, U. *J. Solid State Chem.* **1979**, *29*, 379;
(3) Rabenau, A. *Solid State Ionics* **1982**, *6*, 277.
(4) Gregory, D. H. *Coord. Chem. Rev.* **2001**, *215*, 301.
(5) Rabenau, A.; Schulz, H. *J. Less-Common Met.* **1976**, *50*, 155.
(6) Schulz, H.; Schwarz, K.-H. *Acta Crystallogr., Sect. A* **1978**, *34*, 999.
(7) Schulz, H.; Thiemann, K. H. *Acta Crystallogr., Sect. A* **1979**, *35*, 309.
(8) Zucker, U. H.; Schulz, H. *Acta Crystallogr., Sect. A* **1982**, *38*, 568.
(9) Nishijima, N.; Takeda, Y.; Imanishi, N.; Yamamoto, O.; Takano, M. *J. Solid State Chem.* **1994**, *113*, 205.
(10) Bhamra, M. S.; Fray, D. J. *J. Mater. Sci.* **1995**, *30*, 5381.
(11) Asai, T.; Nishida, K.; Kawai, S. *Mater. Res. Bull.* **1984**, *19*, 1377.
(12) Martem'yanov, N. A.; Tamm, V. Kh.; Obrosov, V. P.; Martem'yanova, Z. S. *Inorg. Mater.* **1995**, *31*, 65.
(13) Nishijima, M.; Kagohashi, T.; Imanishi, M.; Takeda, Y.; Yamamoto, O.; Kondo, S. *Solid State Ionics* **1996**, *83*, 107.
(14) Nishijima, M.; Kagohashi, T.; Takeda, Y.; Imanishi, M.; Yamamoto, O. *J. Power Sources* **1997**, *68*, 510.
(15) Shodai, T.; Okada, S.; Tobishima, S.; Yamaki, J. *J. Power Sources* **1997**, *68*, 515.

10.1021/cm010718t CCC: $22.00 
Published on Web 04/27/2002

In fact, reactions of $Li_3N$ with the first row transition elements were among the first studies performed in nitride chemistry over 50 years ago.[17−19] The $Li_3N$-type ternary nitrides were observed to form for M = Co, Ni, and Cu in solid solutions of limited range (typically $x < 0.5$).[18] Substitution is ostensibly isovalent ($M^+$ for $Li^+$) on two-coordinate sites. The electrochemical performance of these α-$Li_3N$-type compounds might be tailored via increased stability and/or conductivity; the latter achieved through reduced activation energies and/or increased charge carrier concentration. In recent studies, we and others have shown that ternary compounds of this type can be synthesized containing levels of $Li^+$ vacancies higher than the 1−2% found in $Li_3N$, with corresponding implications for redox chemistry, conductivity, and magnetism.[20−23] The vacancies in these $Li_{3-x-y}M_xN$ compounds (or $Li_{3-x-y}M_x\square_yN$ where □ is a vacancy) may be either ordered or disordered within the $Li_3N$-type structure. There is a drive to both develop the synthetic routes toward new compounds of this type and to fully characterize these potential materials in terms of structure and bonding, redox chemistry, electronic, and transport properties. Significant changes are to be expected by the replacement of lithium with transition metals and the possibilities also of crystal growth in these systems offer the potential for systematic anisotropic property measurements.

As part of our studies of the synthesis of nitrides in Li/M/N systems (M = late transition metal) and comprehensive examination of structure and properties, we report here the results of powder neutron diffraction investigations of $Li_3N$ and substituted nickel and copper nitrides. These structural investigations show that the substitution of transition metals is aliovalent and that the replacement of $Li^+$ by $M^{2+}$ creates levels of $Li^+$ vacancies in ternary compounds much higher than those observed in the parent nitride. The detailed structural picture so-revealed suggests that these ternary compounds contain highly mobile $Li^+$ ions within Li−N layers. These layers are, in turn, more tightly bound to one another as a result of transition-metal substitution.

## Experimental Section

**Synthesis of $Li_3N$.** The binary starting material $Li_3N$ was synthesized by the reaction of the molten alkali metal−sodium alloy with dried nitrogen at 650 °C. Molten alkali metals are highly reactive to air and water and melts were handled in inert atmospheres at all times. The cleaned metal (Alfa, 99+%) was added to molten sodium (Aldrich, 99.95%) in a purified Argon-filled evacuable glovebox. The cooled crucible of alloy was heated in a stainless steel vessel under a positive pressure of nitrogen, monitored by a pressure transducer, until the gas pressure remained constant (ca. 48−72 h). Excess sodium was then removed by vacuum distillation at 350−400 °C for 24 h. Liquid sodium is unreactive toward nitrogen and serves as an inert solvent for lithium. The reaction yielded polycrystalline samples of red-purple $Li_3N$. The identity of the powder as highly crystalline α-$Li_3N$ was confirmed by powder X-ray diffraction (PXD) (ICDD card No. 30-759) with negligible alkali metal oxide impurity in the products.

**Synthesis of Ternary Nitrides.** All manipulations were performed in a nitrogen-filled recirculating glovebox (Saffron Scientific; <5 ppm $H_2O$, <1 ppm $O_2$). Crystalline powders of ternary nitrides were prepared by reaction of $Li_3N$ with cleaned copper foil (Alfa 99.9%; 0.127-mm thickness) or nickel foil (BDH 99.9%; 0.15-mm thickness) tubes. Foils were cleaned by reduction under 20% $H_2/N_2$ gas for 16 h at 600 °C. This was essential to remove surface oxide. Reactions performed without the cleaning step produced large amounts of $Li_2O$ at the tube interface, which permeated into the bulk. Tubes were filled with $Li_3N$ powder, placed inside a stainless steel crucible, sealed in a stainless steel vessel under positive $N_2$ pressure, and heated at 750 °C for 5 days. Reactions yielded thick, highly crystalline films on the surface of the foils, which were gold (nickel) or dark blue/black (copper) in color. Excess $Li_3N$ remained as blocks of calcined powder and was easily separated from the products in each case. The identity of the excess binary nitride was confirmed by PXD. Bulk quantities of the crystalline ternary solids were easily removed from the surface of the metals by gentle flexing. Single crystals from this film of air-sensitive material were selected by inspection under an optical microscope in a nitrogen-filled glovebox, isolated, and data-collected from crystals sealed in capillaries at 298 K. Preliminary reports of the diffraction data collected from single crystals appear elsewhere and more detailed discussions of structure solutions will be published in due course.[23] Products were sensitive to moist air and hydrolyzed readily with water to yield ammonia gas.

**Characterization by PXD.** PXD data were collected using a Philips XPERT $\theta-2\theta$ diffractometer with Cu Kα radiation. Data for air-sensitive materials were collected using custom-designed sealed sample holders.[24] Phase purity was evaluated from short scans (ca. 1 h) over 5°−80° $2\theta$ using the PC-IDENTIFY routine (accessing the ICDD database). Samples were indexed and cell parameters refined using DICVOL91[25] followed by least-squares fitting. PXD patterns from bulk products were compared with diffraction patterns generated from our single-crystal data using POWDERCELL 2.3.[26]

**Powder Neutron Diffraction (PND) Data Collection and Structure Refinement.** Time-of-flight (TOF) PND data were collected for ca. 1-g samples of $Li_{3-y}N$ (**1**), $Li_{2.6-y}Cu_{0.4}N$ (**2**), and $Li_{2.2-y}Ni_{0.8}N$ (**3**) using the Special Environment Powder Diffractometer (SEPD) at the Intense Pulsed Neutron Source (IPNS), Argonne National Laboratory.[27] Diffraction data were collected on all detector banks. However, only the high-resolution backscattering data ($\Delta d/d = 0.035$, $0.5 < d < 3.35$ Å) are presented here. The air-sensitive samples were initially loaded in 8-mm diameter, thin-walled, silica tubes in a nitrogen-filled recirculating glovebox and subsequently sealed under vacuum. These sealed silica ampules were contained in vanadium cans during neutron diffraction data collection.

Rietveld refinements were performed using the General Structure Analysis System.[28] Starting models were taken as the published single-crystal X-ray diffraction (XRD) structure of α-$Li_3N$ and structures of $Li_{2.48}Cu_{0.4}N$ and $Li_{1.78}Ni_{0.78}N$ refined earlier from our own single-crystal data respectively for **1**, **2**, and **3**.[23] Initial refinements thus considered solutions in

(16) Takeda, Y.; Nishijima, M.; Yamahata, M.; Takeda, K.; Imanishi, N.; Yamamoto, O. *Solid State Ionics* **2000**, *130*, 61.
(17) (a) Juza, R.; Hund, F. *Z. Anorg. Allg. Chem.* **1948**, *257*, 1. (b) Juza, R.; Weber, H. H.; Meyer-Simon, E. *Z. Anorg. Allg. Chem.* **1953**, *273*, 48.
(18) Sachsze, W.; Juza, R. *Z. Anorg. Allg. Chem.* **1949**, *259*, 278.
(19) Juza, R.; Langer, K.; von Benda, K. *Angew. Chem.* **1968**, *80*, 373; *Angew. Chem., Int. Ed. Engl.* **1968**, *7*, 360.
(20) Klatyk, J.; Höhn, P.; Kniep, R. *Z. Kristallogr.* **1998**, *213*, 31.
(21) Barker, M. G.; Blake, A. J.; Edwards, P. P.; Gregory, D. H.; Hamor, T. A.; Siddons, D. J.; Smith, S. E. *Chem. Commun.* **1999**, 1187.
(22) Weller, M. T.; Dann, S. E.; Henry P. F.; Currie, D. B. *J. Mater. Chem.* **1999**, *9*, 283.
(23) Gregory, D. H.; O'Meara, P. M.; Gordon, A. G.; Siddons, D. J.; Blake, A. J.; Barker, M. G.; Hamor, T. A.; Edwards P. P. *J. Alloys Compd.* **2001**, *317−318*, 237.
(24) Barker, M. G.; Begley, M. J.; Edwards, P. P.; Gregory, D. H.; Smith, S. E. *J. Chem. Soc., Dalton Trans.* **1996**, 1.
(25) Boultif, A.; Louer, D. *J. Appl. Crystallogr.* **1991**, *24*, 987.
(26) Nolze G.; Kraus, W. *Powder Diffr.* **1998**, *13*, 256.
(27) Jorgensen, J. D.; Faber, J. J.; Carpenter, J. M.; Crawford, R. K.; Haumann, J. R.; Hittermann, R. L.; Kleb, R.; Ostrowski, G. E.; Rotella, F. J.; Worlton T. G. *J. Appl. Crystallogr.* **1989**, *22*, 321.
(28) Larson, A. C.; von Dreele, R. B. *The General Structure Analysis System*; Los Alamos National Laboratories, Report LAUR 086-748; LANL: Los Alamos, NM, 1999.

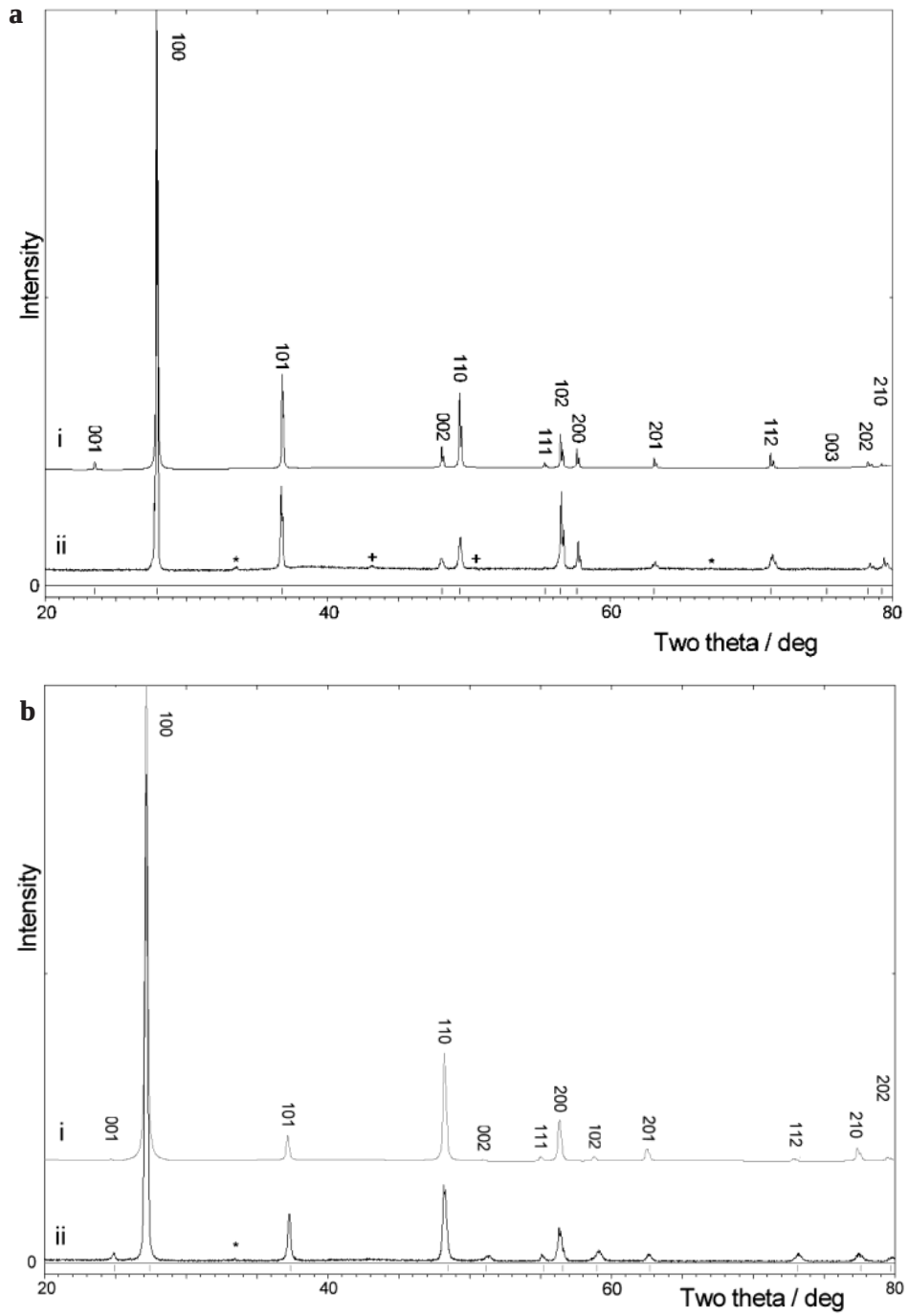


**Figure 1.** Calculated (i) and observed (ii) profiles for (a) $Li_{2.6-y}Cu_{0.4}N$ and (b) $Li_{2.2-y}Ni_{0.8}N$ generated by POWDERCELL 2.3 from experimental PXD data vs model single-crystal data. Also indicated are peaks due to $Li_2O$ (*) and Cu (+).

hexagonal space group *P*6/*mmm* (No. 191). Peak shapes were modeled in each case using TOF profile function no. 3 (convolution of back-to-back exponentials with a pseudo-Voigt function). The silica ampules generated a significant noncrystalline scattering contribution to the diffraction data. This amorphous scattering contribution was fitted as background using the reciprocal interpolation function (no. 8 within GSAS). Initial cycles allowed for the variation of the scale, background, linear absorption, and lattice parameters. As the refinements progressed, strain broadening peak profile parameters and isotropic temperature factors were introduced. Lithium oxide ($Li_2O$) was simultaneously refined as an impurity phase in each case and nickel metal was also refined for sample **3**. Copper metal was initially introduced as an additional phase in **2** as had been indicated by PXD (see below). Little evidence was seen for Cu in the PND profile, however, and phase fractions for Cu consistently refined to negative values. It was therefore omitted as an impurity phase in the final solution and was assumed to have been a localized impurity, removed from the copper foil, exclusively in the PXD sample.

Once initial stabilization of the refinement had been achieved, the occupancy of the interplanar Li−M 1b site $(0,0,{}^1/_2)$ was freed in **2** and **3**. The occupancy of this 1b site in **2** and **3** converged smoothly to values in close agreement with single-crystal XRD data.[23] The occupancy of the Li(2) 2c site $({}^1/_3,{}^2/_3,0)$ was refined for all three compositions. Inclusion of anisotropic temperature factors in the refinement yielded the final structures reported in this paper. For **2** the anisotropic temperature factors of the 1b site refined very close to zero when simultaneously refined with site occupancy. In final cycles, the 1b site occupancy was fixed (at the previously convergent value and in agreement with single-crystal data) and anisotropic temperature factors were allowed to converge to physically meaningful values.

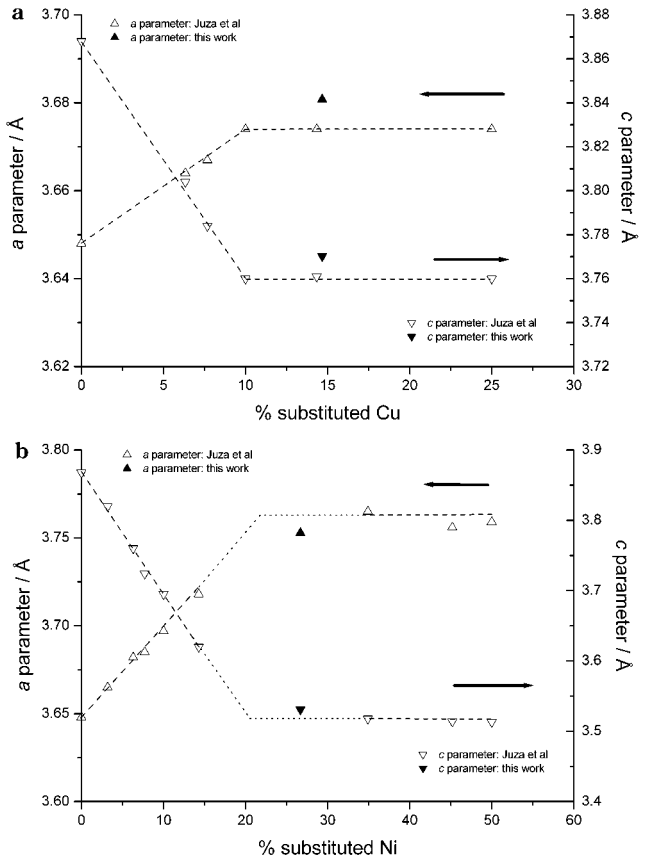


**Figure 2.** Plots of (a) *a* and *c* parameters vs percentage copper content in $Li_{3-x-y}Cu_xN$ and (b) *a* and *c* parameters vs percentage nickel content in $Li_{3-x-y}Ni_xN$. Data from Sachsze and Juza (ref 18) are denoted by open triangles. Data from this work are denoted by filled triangles. The trend lines are taken from ref 18.

Previous reports investigating relations between structure and properties in α-$Li_3N$ suggest that charge balance is maintained by partial substitution of H for Li. More accurately, $Li^+$ vacancies are therefore created by partial substitution of nitride, $N^{3-}$ by imide $NH^{2-}$. Deliberately, deuterium-doped $Li_{2.95}ND_{0.01}$ was previously investigated by single-crystal neutron diffraction, revealing the 6j position ($x$,0,0) $x \approx 0.28$ to be ca. 0.2% occupied.[29] The possibility of H substitution on Li positions or on the 6j site was investigated, but in all cases occupancies refined to zero. It remains possible that very low levels of H may be substituted. Given the strong amorphous diffraction component arising from the silica ampules, any sign of H from incoherent scattering was impossible to detect.

Other compensating mechanisms for lithium vacancy creation were explored, namely, the possibilities of nonstoichiometry at the nitrogen site ($Li_{3-x}N_{1-x/3}$) or partial substitution of oxide, $O^{2-}$, for nitride ($Li_{3-x}N_{1-x}O_x$). Attempts to vary the N occupancy resulted in physically meaningless values slightly above full occupation (1.004). Efforts to replace $N^{3-}$ with $O^{2-}$ at the 1a site led to a marginal increase in $R_{wp}$ (from 0.0392 to 0.0394) and produced N occupancies slightly above 1 (1.001) and a corresponding negative O occupancy (−0.001). These alternatives were thus rejected in the final model, and given that $Li_{3-x}N$ is not an electronic conductor, imide substitution seems the most likely mechanism for compensating $Li^+$ vacancies.

Considering the higher level of refined lithium vacancies in **3** (compared to **1** and **2**) and the precedence for Li vacancy ordering in the Li−Ni−N system,[20,21] an alternative ordered model in space group $P\bar{6}m2$ (No. 187) was also evaluated using the structure of LiNiN as a basis.[21] The calculated diffraction patterns from the $P6/mmm$ and $P\bar{6}m2$ space groups are almost indistinguishable. No additional reflections are generated in the $P\bar{6}m2$ model. The refinement was performed in an identical fashion to those above with the exception that the occupancies of the now-inequivalent Li positions within the nominal $[Li_2N]$ plane, 1e ($^2/_3$,$^1/_3$,0) and 1f ($^1/_3$,$^2/_3$,0) (vacant in LiNiN) were refined independently. Differences in final residuals and fit between the solution in this space group and the disordered variant in $P6/mmm$ were negligible. However, the disordered ($P6/mmm$) solution was favored based on the final stoichiometry and vacancy distribution. In these respects, first the solution in $P\bar{6}m2$ yielded a slightly higher level of substitution of Ni at the interplanar 1b site ($x \approx 0.85$ cf. $x \approx 0.78$ from single-crystal data) and second the Li occupancy of the 1e site refined consistently to values higher than 1. Overall, there was no evidence to justify the $P\bar{6}m2$ model over the higher symmetry $P6/mmm$ solution.

## Results and Discussion

X-ray powder data for the transition-metal-substituted phases revealed bulk samples of almost phase-pure ternary compounds. Small amounts of lithium oxide and transition metal were observed in each PXD sample. The former impurity most likely originates from either partial reaction of the nitride during handling and/or from the starting material $Li_3N$. The transition-metal impurities, present in very low concentrations, probably derive from the containing foil as the crystalline product is removed. The experimental powder patterns of the ternary compounds are in excellent agreement with calculated patterns generated from our single-crystal XRD data (Figure 1) from crystals extracted from the same reaction.[23]

PXD patterns of the nitridometalates were indexed in space group $P6/mmm$ with lattice parameters $a$ = 3.652(1) Å, $c$ = 3.872(1) Å, $a$ = 3.680(1) Å, $c$ = 3.770(1) Å, and $a$ = 3.763(1) Å, $c$ = 3.531(1) Å, for **1**, **2**, and **3**, respectively. The nominal transition-metal contents of the ternary compounds are higher than previously reported at near-ambient pressures and exceed the solubility limits originally defined by Sachsze and Juza.[18] Plots of the cell parameters versus transition-metal substituent level are shown in Figure 2 with the new ternary compounds reported here overlaid on Sachsze and Juza's original graphs. The new compositions appear to clearly extend the perceived solid solutions in both the Li−Cu−N and Li−Ni−N systems. In this respect the previous limits were defined at 10% Cu ($x$ = 0.3) and 21% Ni ($x$ = 0.61), respectively. The fit with $x$ is nonlinear across this expanded range, although compounds of lower compositions may need to be re-evaluated not only in terms of substituted M ($x$) but also in terms of Li vacancy levels ($y$) previously assumed to be ca. zero and therefore constant.

Powder neutron diffraction data confirmed that bulk samples were almost single-phase nitrides with **1**, **2**, and **3** containing 6.3, 2.1, and 1.6 wt % of lithium oxide, $Li_2O$, respectively. As noted above, $Li_2O$ almost certainly originates from partial reaction of the nitrides during handling and the relative proportion of the oxide was observed to increase slightly over time. The nitridonickelate (**3**) also contained 0.9 wt % Ni. Observed, calculated, and difference profile plots for the three refinements are shown in Figures 3−5. Crystallographic parameters for the refinements are shown in Table 1. Final atomic parameters from the structure refinements are described in Table 2.

(29) Thomas, J. O.; Tellgren, R. *Solid State Ionics* **1981**, *5*, 407.

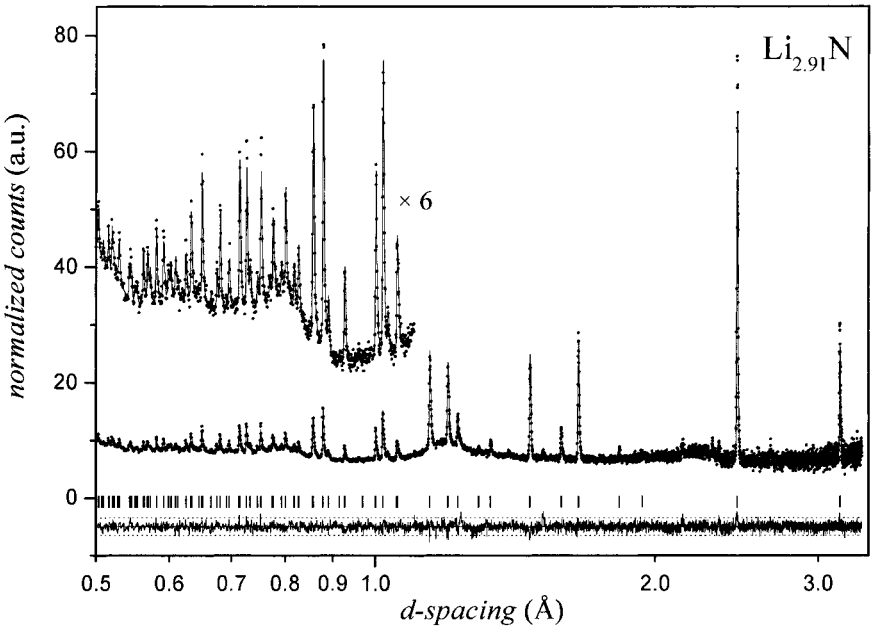


**Figure 3.** Powder neutron diffraction data and Rietveld refinement profile for $Li_{2.91}N$ refined in the *P*6/*mmm* space group. Dots are the normalized observed data and the solid line is the calculated profile. Tick marks below the profile mark the positions of allowed reflections for the $Li_{2.91}N$ phase. The difference between the observed and calculated profiles is plotted at the bottom in units of difference divided by estimated standard deviation. The dotted lines above and below the difference/esd line are +3 and −3 in these units.

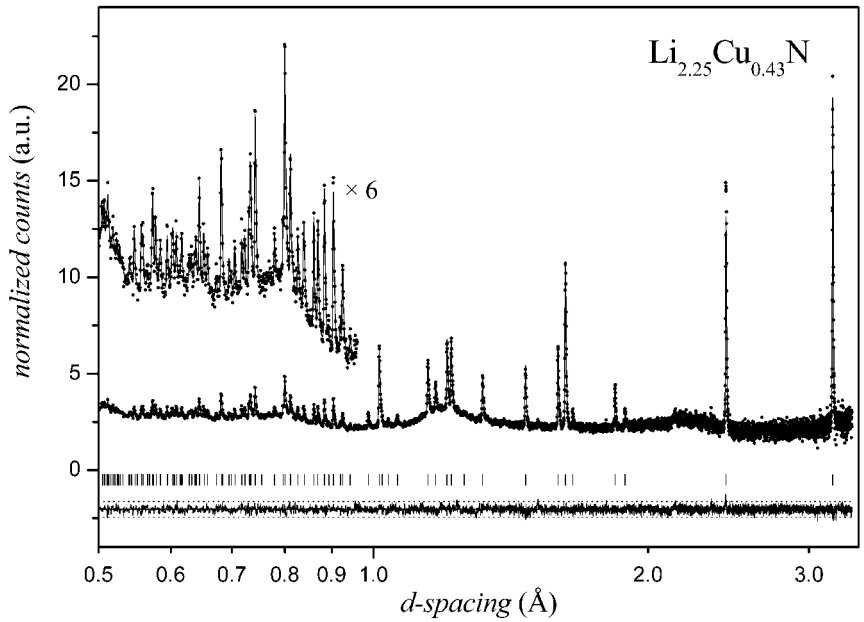


**Figure 4.** Powder neutron diffraction data and Rietveld refinement profile for $Li_{2.21}Cu_{0.40}N$ refined in the *P*6/*mmm* space group. Format is the same as that for Figure 3.

The refined structure of lithium nitride, α-$Li_3N$, is thus, essentially, as previously reported.[5] Lithium occupies two positions: Li(1), the two-coordinate 1b site, and Li(2), the three-coordinate 2c site. N occupies the 1a position and is coordinated to six lithium atoms—Li(2)—in the *ab* plane and to two lithium atoms—Li(1)—along *c*. Hence, the structure contains nominal [$Li_2N$] layers parallel to the 001 plane connected via Li atoms along the *c* direction. In terms of coordination polyhedra, N-centered hexagonal bipyramids are connected by edges in the *ab* plane and by vertexes (apexes) along *c*. The structures of the M-substituted compounds described here, $Li_{2.25}Cu_{0.43}N$ and $Li_{1.36}Ni_{0.79}N$, effectively only differ from $Li_3N$ in that the Li(1) site is partially occupied by Cu or Ni. The distribution is disordered and the space group (*P*6/*mmm*) is unchanged as a result of this substitution (Figure 6). The key aspects from our neutron data (and the important differences compared to X-ray structural interpretations) are the location and quantification of lithium vacancies within the binary and ternary nitride structures. In lithium nitride, our refined model describes a Li(2) site that is 96(3) % occupied. This is very close to the value of 98−99% proposed previously from systematic variable temperature single-crystal XRD studies.[7] Our powder neutron diffraction results corroborate that the level of Li vacancies in $Li_3N$ at room temperature is very small, 3(2)%. If imide substitution was indeed the mechanism

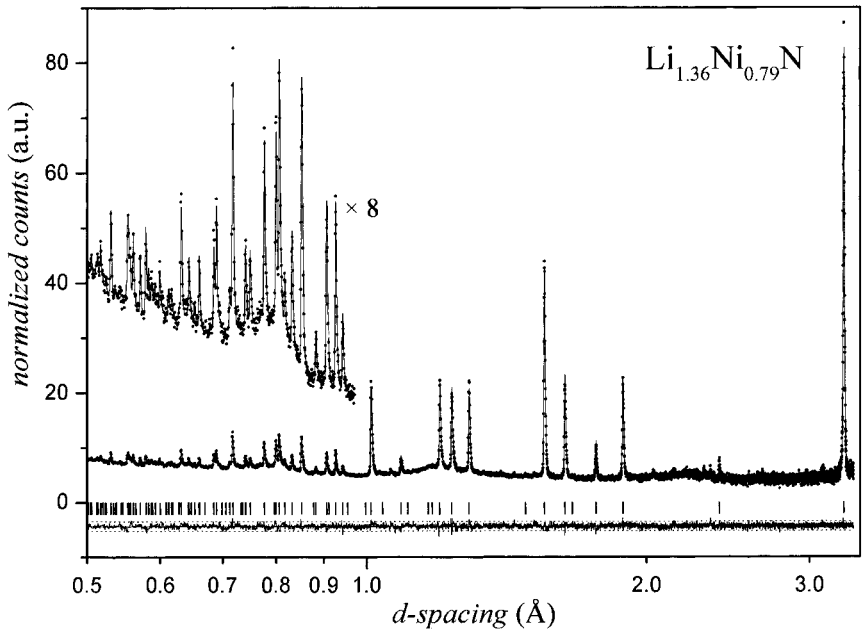


**Figure 5.** Powder neutron diffraction data and Rietveld refinement profile for $Li_{1.36}Ni_{0.79}N$ refined in the *P*6/*mmm* space group. Format is the same as that for Figure 3.

**Table 1. Crystallographic Data for $Li_{3-x-y}M_xN$ Compounds**

| formula | $Li_{2.91}N$ | $Li_{2.25}Cu_{0.43}N$ | $Li_{1.36}Ni_{0.79}N$ |
|---|---|---|---|
| instrument | SEPD, IPNS, Argonne | | |
| radiation | ToF neutron | | |
| temperature/K | 298 | | |
| crystal system | hexagonal | | |
| space group | *P*6/*mmm* (No. 191) | | |
| *Z* | 1 | | |
| *M* | 34.22 | 56.80 | 69.82 |
| calculated density, $\rho$/g cm$^{-3}$ | 1.266 | 2.133 | 2.672 |
| unit cell dimensions: | | | |
| *a*/Å | 3.6576(1) | 3.6791(1) | 3.7696(1) |
| *c*/Å | 3.8735(1) | 3.7725(1) | 3.5270(1) |
| *V*/Å$^3$ | 44.879(1) | 44.221(1) | 43.406(1) |
| ratio *c*/*a* | 1.06 | 1.03 | 0.94 |
| observations, parameters | 4253, 50 | 4253, 50 | 4253, 54 |
| $\chi^2$ | 1.361 | 1.222 | 1.394 |
| $R_{wp}$ | 0.0392 | 0.0371 | 0.0369 |
| $R_p$ | 0.0262 | 0.0245 | 0.0251 |
| $R_{Bragg}$ | 0.0585 | 0.0539 | 0.0619 |

**Table 2. Final Atomic Parameters for $Li_{3-x-y}M_xN$ Compounds[a]**

| | $Li_{2.91}N$ | $Li_{2.25}Cu_{0.43}N$ | $Li_{1.36}Ni_{0.79}N$ |
|---|---|---|---|
| | (Li,M)1 (1b) (0,0,$^1/_2$) | | |
| M SOF[b] | 0 | 0.43 | 0.79(1) |
| 100 × $U_{11}$/Å$^2$ | 3.1(2) | 0.56(7) | 1.8(1) |
| 100 × $U_{33}$/Å$^2$ | 2.7(2) | 0.13(12) | 0.6(2) |
| 100 × $U_{12}$/Å$^2$ | 1.6(1) | 0.28(4) | 0.9(1) |
| | Li2 (2c) ($^2/_3$,$^1/_3$,0) | | |
| SOF | 0.96(3) | 0.84(2) | 0.57(2) |
| 100 × $U_{11}$/Å$^2$ | 2.2(1) | 1.6(2) | 3.5(4) |
| 100 × $U_{33}$/Å$^2$ | 4.4(3) | 4.6(3) | 5.5(5) |
| 100 × $U_{12}$/Å$^2$ | 1.1(1) | 0.8(1) | 1.7(1) |
| | N (1a) (0,0,0) | | |
| SOF | 1.0 | 1.0 | 1.0 |
| 100 × $U_{11}$/Å$^2$ | 0.97(3) | 0.98(3) | 2.5(1) |
| 100 × $U_{33}$/Å$^2$ | 1.30(5) | 0.78(4) | 0.6(1) |
| 100 × $U_{12}$/Å$^2$ | 0.48(2) | 0.49(2) | 1.2(1) |

[a] $U_{eq} = {}^4/_3[a^2U_{11} + b^2U_{22} + c^2U_{33} + ab(\cos\gamma)U_{12} + ac(\cos\beta)U_{13} + bc(\cos\alpha)U_{23}]$. $U_{11} = U_{22} = 2U_{12}$; $U_{13} = U_{23} = 0$ for all atomic positions. [b] Li SOF (site occupancy factor) = 1 − M SOF.

by which charge balance is achieved, this would correspond to a nominal composition of $Li_{2.91}NH_{0.09}$. Prompt gamma activation analysis (PGAA) would be perhaps the most accurate way of determining such low H concentrations in this system.

The powder neutron diffraction data for the ternary nitridometalates first confirm high levels of transition-metal substitution, in very good agreement with our single-crystal data, and second indicate much higher levels of lithium vacancies in the ternary compounds than in $Li_3N$.[7] PND accurately quantifies these vacancies and reveals that these levels are higher than previously described by XRD data for crystals of nominally the same products.[23] The compositions $Li_{2.25}Cu_{0.43}N$ and $Li_{1.36}Ni_{0.79}N$ suggest transition-metal valences of 1.7 and 2.1 for Cu and Ni, respectively. These results are consistent with the aliovalent replacement of interplanar $Li^+$ with $M^{2+}$. Hence, for M = Cu (**2**), $x$ = 0.43, $y$ = 0.32, and for M = Ni (**3**), $x$ = 0.79, $y$ = 0.85, and in each case the general nitridometalate stoichiometry across the solid solutions approaches $Li_{3-2x}M_xN$ (i.e., $(Li_{1-x}M_x)[(Li_{2-x}\square_x)N]$ where □ is a Li vacancy). This

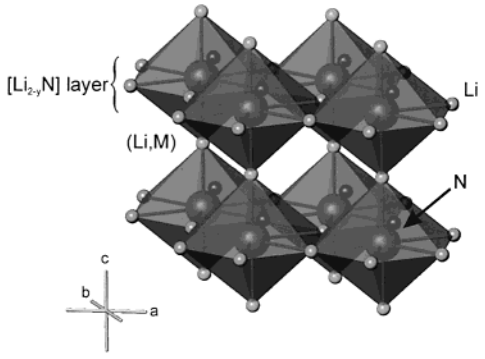


**Figure 6.** Structure of $Li_{3-x-y}M_xN$. Polyhedral representation showing layers of edge-sharing $NLi_6(Li,M)_2$ hexagonal bipyramids linked by vertexes along the *c* axis. The $[Li_{2-y}N]$ planes are also highlighted.

is especially notable for M = Ni and the previously reported ordered nitridonickelate LiNiN also fits into this general formulation.[21] The ordered nitridonickelates with (~2*a* × ~2*a* × *c*) doubled superstructures,

**Table 3. Selected Interatomic Distances and Angles for $Li_{3-x-y}M_xN$ Compounds**

| compound | $Li_{2.91}N$ | $Li_{2.25}Cu_{0.43}N$ | $Li_{1.36}Ni_{0.79}N$ |
|---|---|---|---|
| (Li,M)(1)−N ×2/Å | 1.9368(1) | 1.8863(1) | 1.7635(1) |
| Li(2)−N ×3/Å | 2.1117(1) | 2.1241(1) | 2.1764(1) |
| Li(2)−Li(2) ×3/Å | 2.1117(1) | 2.1241(1) | 2.1764(1) |
| Li(2)−(Li,M)(1) ×6/Å | 2.8654(1) | 2.8407(1) | 2.8012(1) |
| (Li,M)(1)−N−(Li,M)(1) ×3/deg | 180 | 180 | 180 |
| Li(2)−N−Li(2)/deg | 120 | 120 | 120 |

$Li_5Ni_3N_3$ and $Li_{5.69}Ni_{2.31}N_3$,[20,21] possess lower *y*:*x* ratios and may be either genuine mixed valence ($Ni^+/Ni^{2+}$) compounds or be incompletely elucidated in terms of Li stoichiometry (as obtained from XRD). The premise of substitution of divalent transition metals, certainly in disordered nitridometalates, also agrees with our preliminary magnetic measurements of Li−Cu−N compounds where we observe effective moments representative of $Cu^{2+}$.[30] Further magnetic studies of Li−M−N (M = Co, Ni, Cu) compounds are in progress.

Important interatomic distances and angles are described in Table 3. The two equal interplanar (Li,M)(1)−N bond lengths are the shortest of the metal−nitrogen distances in all three compounds and reduce as the transition-metal substitution level, *x*, increases. This reduction probably reflects the increased covalency ($\pi$-character) of late transition-metal−nitrogen bonds over alkali metal−nitrogen bonds, as seen in the majority of Cu and Ni nitrides.[31−33] By contrast, the intraplanar Li(2)−N bonds lengthen with *x* and also, perhaps more significantly for this distance, with Li vacancy level, *y*. These trends in the two metal−nitrogen bond lengths are thus consistent with the observed decrease in *c* parameter and the *ab* plane expansion with increasing *x* and *y*. These observations thus support the strengthening of the (Li,M)(1)−N bond and the weakening of the Li(2)−N bond with increased transition-metal substitution and vacancy creation, qualitatively fitting the results of Sachsze and Juza in the Li−M−N (M = Co, Ni, Cu) systems and consistent also with more recent electrochemical results.[11,13] Note that expansion of the *ab* plane also occurs as *y* apparently increases with temperature in $Li_3N$ itself (deviating nonlinearly with temperature above 570 K).[7]

The metal−nitrogen distances in $Li_3N$ are close to those originally reported from single-crystal data (1.939 and 2.106 Å for Li(1)−N and Li(2)−N, respectively).[5] There is a marginal increase in the *a* parameter and Li(2)−N distance in our data, which may again correlate with *y* (reported as nominally zero in the single-crystal study). The (Li,M)1−N distances are close in value to bond distances in other ternary nitrides where these metals are linearly coordinated (e.g., 1.7904 Å in CaNiN and 1.883(13) and 1.858(13) Å in SrCuN).[33,34] Interestingly, despite partial occupation of the interplanar site by larger $Li^+$, the bond lengths are shorter than those seen in the binary M(I) compounds, $Ni_3N$ and $Cu_3N$

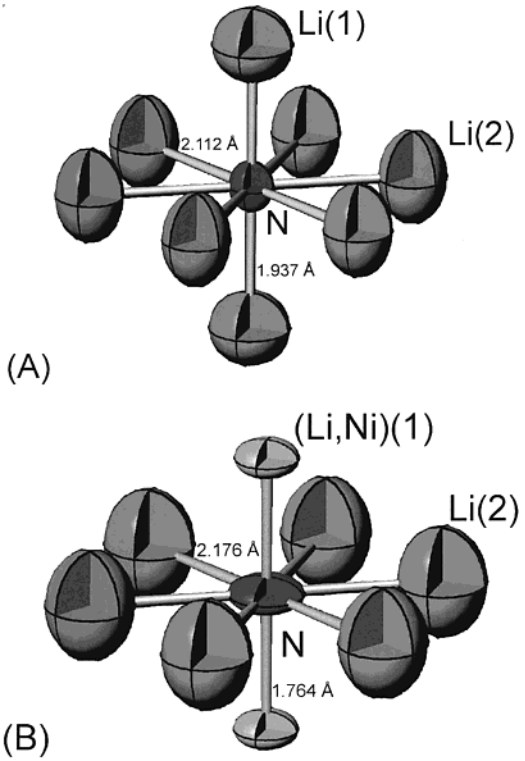


**Figure 7.** Coordination environment around nitrogen in (a) $Li_3N$ and (b) $Li_{1.36}Ni_{0.79}N$.

(1.877 and 1.910 Å, respectively).[35,36] There is only one Ni(II) nitride reported outside the Li−Ni−N system, $Sr_2NiN_2$.[37] This compound has a shortest Ni−N bonding distance of 1.59(3) Å and an average bond length of ca. 1.83 Å on the basis of one of two models incorporating split Ni and N sites. By this comparison, the short (Li,M)−N bonds in the $Li_{3-x-y}M_xN$ compounds signify M(II) substitution as postulated, although it should be noted that perceived increased covalency ($\pi$-bonding), even in ternary M(I) compounds, significantly reduces metal−nitrogen bonding distances relative to the ionic radii[38] (and to distances in binary group 10 and 11 nitrides). Bond valence sums calculated for each of the cation and anion sites in an array of $Li_{3-x-y}M_xN$-type compounds are shown in Table 4.[39] Only semiquantitative arguments can be made on the basis of these data, given that the sums for Li are consistently smaller than expected (even in $Li_3N$) and that, as yet, there are no reliable $R_{ij}$ values for Ni and Cu in oxidation states above I in nitrides. However, several trends are readily apparent: first, valence sums for Li(2) are always below 1 and smaller in doped compounds with increased vacancy concentration, *y*; second, (Li,M)(1) *V* values increase with M substitution (*x*), relative to $Li_3N$, consistent with partial replacement of $Li^+$ by $M^{2+}$. Values for calculated (Li,M) site valences are in variable agreement with stoichiometry for $Li_{3-x-y}M_xN$ ($x < 3$), emphasizing the sensitivity of $R_{ij}$ values with M oxidation state (as also observed for example for Cu in oxides

(30) Gordon, A. G.; Gregory, D. H.; Blake, A. J.; Weston, D. P.; Jones, M. O. *Int. J. Inorg. Mater.* **2001**, *3*, 973.
(31) Brese, N. E.; O'Keeffe, M. *Struct. Bond. (Berlin)* **1992**, *79*, 305.
(32) Niewa, R.; DiSalvo, F. J. *J. Alloys Compd.* **1998**, *279*, 153.
(33) Chern, M. Y.; DiSalvo, F. J. *J. Solid State Chem.* **1990**, *88*, 459.
(34) DiSalvo, F. J.; Trail, S. S.; Yamane, H.; Brese, N. E. *J. Alloys Compd.* **1997**, *255*, 122.
(35) Juza, R.; Sachsze, W. *Z. Anorg. Allg. Chem.* **1943**, *251*, 201.
(36) Juza, R. *Z. Anorg. Allg. Chem.* **1941**, *248*, 118.
(37) Kowach, G. R.; Brese, N. E.; Bolle, U. M.; Warren, C. J.; DiSalvo, F. J. *J. Solid State Chem.* **2000**, *154*, 542.
(38) Baur, W. H. *Crystallogr. Rev.* **1987**, *1*, 59.
(39) Brese, N. E.; O'Keeffe, M. *Acta Crystallogr., Sect. B* **1991**, *47*, 192.

**Table 4. Calculated Site Valences (*V*) in $Li_{3-x-y}M_xN$ Nitrides**

| nitride, $Li_{3-x-y}MN$ | M content, *x* | Li vacancy level, *y* | nominal M ox. state | *V* (Li,M) | *V* (Li) | *V* (N) | derived from reference |
|---|---|---|---|---|---|---|---|
| $Li_{2.91}N$ | 0 | 0.09 | | 0.9 | 0.8 | 2.4 | this work |
| $Li_3N$ | 0 | | | 0.8 | 0.8 | 2.5 | 5 |
| $Li_{2.25}Cu_{0.43}N$ | 0.43 | 0.32 | 1.7 | 1.0 | 0.7 | 2.5 | this work |
| $Li_{2.20}Cu_{0.52}N$ | 0.52 | 0.28 | 1.5 | 1.0 | 0.7 | 2.5 | 22 |
| $Li_{5.69}Ni_{2.31}N_3$ | 0.77 | 0.33 | 1.4 | 1.7 | 0.7/0.9 | 3.2 | 20 |
| $Li_{1.36}Ni_{0.79}N$ | 0.79 | 0.85 | 2.1 | 1.8 | 0.6 | 3.0 | this work |
| $Li_5Ni_3N_3$ | 1 | 0.33 | 1.3 | 1.9 | 0.7/0.8 | 3.0 | 24 |
| LiNiN | 1 | 1 | 2.0 | 1.9 | 0.7 | 2.6 | 24 |
| $Ni_3N$[a] | 3 | 0 | 1.0 | 1.4 | | 4.3 | 35 |
| $Cu_3N$[a] | 3 | 0 | 1.0 | 0.9 | | 2.7 | 36 |

[a] The binary transition-metal nitrides do not crystallize with the α-$Li_3N$ structure; $Ni_3N$−$\epsilon$-$Fe_3N$ structure type, $Cu_3N$−anti-$ReO_3$ structure type.

and fluorides) and, of course, the relative paucity of structural data for Cu and Ni nitrides in defining these parameters. The values also suggest that, in ordered $[Li_{3-x-y}Ni_xN]_3$ nitrides, Li vacancy levels may be higher than those detected by X-ray diffraction (with a commensurate increase in Ni oxidation state).

The coordination geometry around nitrogen in each of the nitrides is in many ways similar and the arrangement around N in **1** and **3** is illustrated in Figure 7. The hexagonal bipyramidal geometry in $Li_3N$ is retained by nitrogen in the $Li_{3-x-y}M_xN$ compounds, but as manifested in the *c*-axis contraction and *ab* plane expansion, this environment becomes more irregular. The thermal ellipsoids in the metal-substituted phases are loosely similar to those in $Li_3N$. (Li,M)(1) and N ellipsoids become more "flattened" in the *ab* plane and Li(2) ellipsoids remain elongated parallel to the *c*-direction (i.e., perpendicular to the $[Li_2N]$ planes). Following the arguments of Schulz et al. for $Li_3N$,[7,8] given the increased Li(2)−N bond lengths and large Li(2) anisotropic thermal parameters observed in $Li_{3-x-y}M_xN$, $Li^+$ within the $[Li_2N]$ planes should be at least as mobile in the ternary nitridometalates as in α-$Li_3N$. Variable temperature solid-state $^7$Li NMR and ionic conductivity measurements are being initiated to test the $Li^+$ mobility in doped compounds and evaluate activation energies for the two proposed $Li^+$ hopping mechanisms, perpendicular and parallel to the *c*-axis.[2−4]

**Acknowledgment.** D.H.G. thanks the EPSRC for the award of an Advanced Research Fellowship and for their financial support of this work. This work has benefited from the use of the Intense Pulsed Neutron Source at Argonne National Laboratory, funded by the U.S. Department of Energy, Office of Science under Contract W-31-109-Eng-38. J.P.H. wishes to acknowledge the support of the U.S. Department of Energy under Contract DE-AC05-960R22464.

CM010718T